Int. J. Adv. Appl. Math. and Mech. 2(3) (2015) 101 - 118 (ISSN: 2347-2529)

Journal homepage: www.ijaamm.com

IJAAMM

International Journal of Advances in Applied Mathematics and Mechanics

Effects of variable viscosity of nanofluid flow over a permeable wedge embedded in saturated porous medium with chemical reaction and thermal radiation

Research Article

Makungu James[1,*], E.W. Mureithi [2], Dmitry Kuznetsov [3]

[1]*Department of Mathematics, The Nelson Mandela African Institution of Science and Technology (NM-AIST), Tengeru, P.O.BOX 447, Arusha, Tanzania*

[2]*Department of Mathematics, University of Dar es Salaam (UDSM), P.O.BOX 35062, Dar es Salaam, Tanzania*

[3]*Department of Mathematics, The Nelson Mandela African Institution of Science and Technology (NM-AIST), Tengeru, P.O.BOX 447, Arusha, Tanzania*

Received 29 January 2015; accepted (in revised version) 27 February 2015

Abstract: The effects of variable viscosity of nanofluid flow over a permeable wedge embedded in saturated non-Darcy porous medium with chemical reaction and thermal radiation have been studied. The governing partial differential equations are converted into a set of non-linear equations with appropriate dimensionless variables and solved numerically by local non-similarity method initiated by Sparrow and Yu (1971) and the fourth order Runge-Kutta method with shooting method. The numerical solutions for dimensionless velocity, temperature and nanoparticle volume fraction, reduced Nusselt and Sherwood numbers are presented graphically for various parameter values governing the problem. It is observed that, the thermal radiation parameter, reaction rate parameter, the variable viscosity parameter, the non-similarity variable, the inertia parameter and wedge angle parameter are shown to have significant effects on reduced Nusselt and Sherwood numbers at the surface of a vertical wedge.

MSC: 80M20 • 65L120 • 65Mxx • 76D05 • 76D10

Keywords: Porous medium • Viscous dissipation • Nanofluids• Convection • Base fluids • Thermal radiation • Reaction rate • Inertia term

1. Introduction

Investigations of convection heat and mass transfer, under the influence of chemical reaction, viscous dissipation, variable viscosity and thermal radiation on the boundary layer flow of nanofluid within porous media have gained importance in many scientific and engineering applications. Such applications can be found in geothermal reservoir, nuclear reactor cooling, chemical catalytic, microelectronic devices, thermal insulation, energy conservation, underground disposal of nuclear waste material etc. An appropriate number of studies have been reported in the literature focusing on the mixed convection heat and mass transfer in the porous media. Since the early work of Darcy in the nineteenth century, several and intensive studies have been conducted on the laminar flow and heat transfer through porous medium, [1]. Darcy's experiment discovered that, in laminar flow through porous medium, the pressure drop caused by the frictional drag is proportional to the velocity at the low Reynolds number range. The Darcy's experiments leads to a law called Darcy law which states that, the velocity of flow of a liquid through a porous medium due to difference in pressure is proportional to the pressure gradient in the direction of flow. The

* Corresponding author.
E-mail address: jamesm@nm-aist.ac.tz

law is a phenomenologically derived constitutive equation that describes the flow through a porous medium [2] and [3]. However, at higher velocity, high-porosity medium and large Reynolds number, the Darcy model in Darcian medium is not satisfied, and consequently the Forchheimer term is added to the momentum equation to account for the inertia effects in the pressure drop. Due to its important applications in many fields, a full understanding of convective heat and mass transfer by non-Darcy mixed convection flow over a heated vertical wedge surface embedded in nanofluid saturated porous medium is meaningful. Numerical investigation of Dufour and Soret effects on unsteady MHD natural convection flow past vertical plate embedded in non-Darcy porous medium was studied by [4]. A detailed review of convective heat and mass transfer in Darcian and non-Darcian porous medium, including an exhaustive list of references, can be found in the book by Nield and Bejan [5]. Apart from that, nanofluids are fluids created by dispersing nanoparticles with sizes of 1-100nm in diameter in traditional heat transfer fluids such as ethylene glycol, water and oil. [7], studied that fluids such as ethylene glycol, water and oil are poor heat transfer fluids, and therefore an alternative approaches are needed to improve the thermal conductivities of these fluids due to the fact that; the thermal conductivities play the major roles on the heat transfer coefficient between the heat transfer medium and the heat transfer surface. Furthermore, the nanoparticles are engineered from metals or metal oxides. Park and Choi [8], observed that copper or carbon nanotubes with 1% nanoparticle volume fractions increased the thermal conductivity of ethylene glycol or oil by 40% and 150% respectively. In this study, the boundary layer flow of nanofluid adjacent to the heated vertical wedge embedded in the porous medium is analyzed.

Several studies have been carried out by different researchers concerning the flow of fluids in porous media with assumption that, the thermo-physical properties of the fluids remain constant throughout the flow regime. However, it is known that these thermo- physical properties may change significantly with temperature fluctuations. For instance, the viscosity of base fluid (water) decreases by about 240% when the temperature increases from $10\,^{\circ}C$ $\left(\mu = 0.0131 g/cm.s\right)$ to $50\,^{\circ}C$ $\left(\mu = 0.00548 g/cm.s\right)$ [9]. Also, it has been proved that, the inclusion of variable viscosity effect in the analysis, provides different numerical solutions compared with the constant viscosity cases. The effects of variable viscosity on mixed convection heat and mass transfer past a wedge with variable temperature under the use of Darcy model was studied by [10]. [11] studied a chemical reaction on Non-linear boundary layer flow over a porous wedge with variable stream conditions. [13] investigated the free convection flow past an impermeable wedge embedded in nanofluid saturated porous medium with variable viscosity base fluid. The case of a mixed convection boundary layer flow of a base fluid over a vertical wall in a porous medium with exponentially varying fluid viscosity was analyzed in detail by [14] using local non-similarity method.

In all the above studies, the effect of variable viscosity of the fluid flow on the boundary layer adjacent to the heated surface was analyzed in detail. However, in many transport phenomena involved in natural and in engineering applications of heat and mass transfer, the interaction of variable viscosity, chemical reaction and thermal radiation may be observed on the boundary layer flow. The study of these phenomena in the flow regime within the porous media is useful for improving a number of chemical technologies, such as polymer production and food processing [11]. It has showed that the presence of foreign nanoparticles in base fluid causes some kind of chemical reaction within the boundary layer. During a chemical reaction between two species (nanoparticles and base fluids), heat is generated and at the same time construction or destruction of nanoparticles are observed on the boundary layer depending on sign of the rate of chemical reaction. In most of cases of chemical reaction, the reaction rate depends on the concentration of the species itself. A reaction is said to be first order if the rate of reaction is directly proportional to concentration itself. The effects of variable viscosity, heat and mass transfer on non-linear mixed convection flow over a porous wedge with thermal radiation in the presence of homogeneous chemical reaction was investigated by [15]. Interaction of variable viscosity and thermophoresis effects on Darcy mixed convective heat and mass transfer past a wedge in the presence of chemical reaction was studied by [16]. Recently, [17] analyzed the influence of viscous dissipation on free convection in a non-Darcy porous medium saturated with nanofluid in the presence of magnetic field. In their study, they observed that heat transfer rate decreases with the increase of viscous dissipation parameter. [18] presented an analysis for the mixed convective boundary layer flow over a vertical wedge embedded in a porous medium saturated with a nanofluid. In their study, the free convection regime was considered to dominate the forced convection regime. Natural-convection flow of nanofluids over vertical cone embedded in non-Darcy porous media was investigated by [20]. Heat and mass transfer effects on unsteady MHD flow of a chemically reacting fluid past an impulsively started vertical plate with radiation was studied by [32]. [21] investigated the variable viscosity, chemical reaction and thermal stratification effects on mixed convection heat and mass transfer along a semi-infinite vertical plate. [12] used a new approach for local similarity solutions of an unsteady hydromagnetic free convective heat transfer flow along a permeable flat surface.

However, very little attention has been paid to study the significance effects of thermal radiation and viscous dissipation over a vertical wedge embedded in saturated non-Darcy porous with nanofluids. Thermal radiation and viscous dissipation effects on the mixed convection heat and mass transfer of radiating fluid are important in context of space technology and processes involving high temperature. [22] investigated a coupled heat and mass transfer in Darcy-Forchheimer mixed convection from a vertical flat plate embedded in a fluid saturated porous

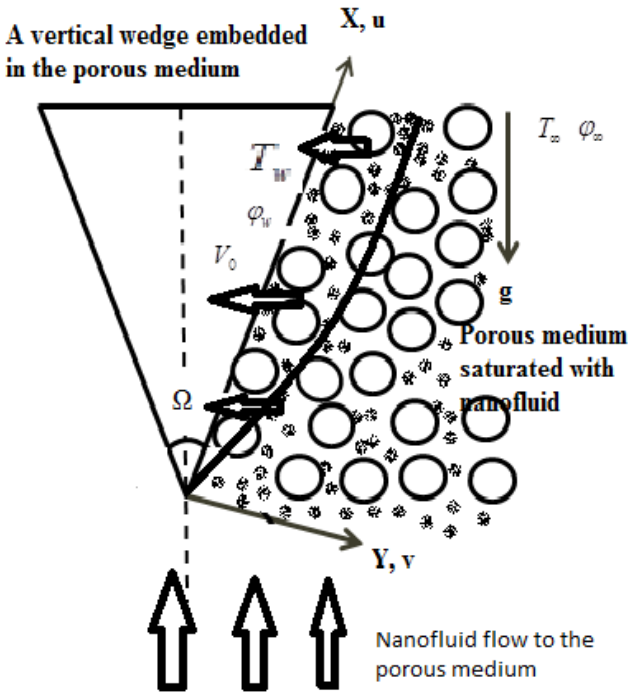

Fig. 1. Physical model and coordinate system.

medium under the effects of radiation and viscous dissipation. On the other hand, the effects of radiation and viscous dissipation on unsteady free convective flow past a moving vertical porous plate embedded in a porous medium was analyzed by [23]. Very recently, [24] analyzed the effects of variable fluid properties on free convection flow and heat transfer at an isothermal vertical plate embedded in a porous medium in the presence of magnetic field and radiation. [25] studied the analysis on variable fluid viscosity of non-Darcian flow over a moving vertical plate in a porous medium with suction and viscous dissipation. The effects of chemical reaction and heat radiation on the MHD flow of viscoelastic fluid through a porous medium over a horizontal stretching flate plate was studied by [26]. Analysis of coupled thermal radiation and viscous dissipation is conducted by several authors (viz., [27]; [19]; [28]; [29]; [6]; [30] etc).

The mentioned literature survey indicates that there is no any study based on boundary layer flow past a vertical wedge embedded in a nanofluid saturated porous medium with variable viscosity of the base fluid, thermal radiation, chemical reaction and viscous dissipation effects. Hence in the study presented here we investigate the effects of variable viscosity of the base fluid, thermal radiation, chemical reaction and viscous dissipation along a vertical wedge embedded in the porous medium. It is assumed that viscosity of the base fluid varies inversely as a linear function of temperature. The problem has an important application to convective flow on the heated vertical wedge, especially in the compact design devices that cannot be cooled by the use of traditional methods rather than using nanoparticle material for enhancing thermal conductivity of the base fluids. Furthermore, the paper is organised in the following manner. Section two presents the problem formulation, Section three is presented the methodology, Section four is presented the numerical technique, Section five will discuss the results and discussion and finally conclusion is made in Section six.

2. Problem Formulation

Let us consider the steady, viscous, incompressible mixed convection boundary layer flow of a nanofluid over a vertical permeable wedge embedded in a porous medium with temperature dependent viscosity, viscous dissipation, chemical reaction and thermal radiation regime. The permeable wedge is placed vertically in the porous medium filled with nanofluid as shown in Fig. 1. The coordinate system is selected in such a way that the x-axis is aligned with the flow on the surface of the vertical wedge and the y-axis is taken normal to it. The system is governed by continuity, momentum, energy and concentration equations in two dimensional laminar flow of nanofluid. The Darcy-Forchheimer model is used to describe the flow of nanofluid in porous medium under free convection dominate regime. As shown in Fig. 1, the slant surface temperature T and the nanoparticle volume fraction take values T_w and φ_w, respectively. The ambient values, attained as y tends to infinity are T_∞ and φ_∞, respectively. It is assumed that the convective nanofluid and the porous medium are in local thermodynamic equilibrium. Also, it is assumed

that the physical properties of the base fluid and that of the nanoparticles are constant except the density of the fluid at the buoyancy term, so that the Oberbeck-Boussinesq approximation holds. In this study, the nanofluid is assumed to be a gray, absorbing-emitting but not scattering medium. Furthermore, the base fluid viscosity varies inversely with temperature and the flow of the nanofluid past a wedge is assumed to satisfy the slip condition. Following the nanofluid equations proposed by [18] together with the boundary layer approximation which is based on a scale analysis and cross differentiation, the basic equations for laminar, steady-state, viscous and incompressible flow can be written as follows;

$$\frac{\partial u}{\partial x}+\frac{\partial v}{\partial y}=0, \tag{1}$$

$$\frac{\partial}{\partial y}\left(\mu(T)\,u\right)+\rho_f F\sqrt{K}\,\frac{\partial}{\partial y}\left(u^2\right)=\left(1-\varphi_\infty\right)\rho_{f\infty}\beta K g_x\frac{\partial T}{\partial y}-\left(\rho_p-\rho_{f\infty}\right)g_x K\frac{\partial \varphi}{\partial y}, \tag{2}$$

$$u\frac{\partial T}{\partial x}+v\frac{\partial T}{\partial y}=\alpha_m\frac{\partial^2 T}{\partial y^2}+\chi\left(D_B\frac{\partial \varphi}{\partial y}\frac{\partial T}{\partial y}+\frac{D_T}{T_\infty}\left(\frac{\partial T}{\partial y}\right)^2\right)+\frac{\mu(T)}{\left(\rho c_p\right)_f}\left(\frac{\partial u}{\partial y}\right)^2-\frac{1}{\left(\rho c_p\right)_f}\frac{\partial q_{ry}''}{\partial y}, \tag{3}$$

$$\frac{1}{\epsilon}\left(u\frac{\partial \varphi}{\partial x}+v\frac{\partial \varphi}{\partial y}\right)=D_B\frac{\partial^2 \varphi}{\partial y^2}+\frac{D_T}{T_\infty}\frac{\partial^2 T}{\partial y^2}-R(x)\left(\varphi-\varphi_\infty\right), \tag{4}$$

where

$$\chi=\frac{\epsilon\left(\rho c_p\right)_p}{\left(\rho c_p\right)_f},\quad \alpha_m=\frac{k_m}{\left(\rho c_p\right)_f}. \tag{5}$$

The Eqns (1) to (4) are subjected to the following boundary conditions;

$$y=0, x\geq 0, v(x,0)=V_w, T(x,0)=T_w, \varphi(x,0)=\varphi_w, \tag{6}$$

$$y\to\infty, x\geq 0, u(x,\infty)=U_\infty, T(x,\infty)=T_\infty, \varphi(x,\infty)=\varphi_\infty. \tag{7}$$

where u and v are the nanofluid velocity components within the porous medium in the direction of x and direction of y, respectively. Whereas, ρ_f, ρ_p, β and $\mu(T)$ are density of the base fluid, density of the nanoparticles, volumetric thermal expansion coefficient and variable dynamic viscosity of the base fluid, ϵ and K are porosity and permeability of the porous medium, T and φ are the temperature and nanoparticle volume fraction in the boundary layer. Furthermore, $\left(\rho c_p\right)_f$, $\left(\rho c_p\right)_p$ and k_m are heat capacitance of the base fluid, heat capacity of the nanoparticles and thermal conductivity of the porous medium, g_x is the acceleration due to gravity component along x-axis, D_B and D_T are the Brownian diffusion coefficient and thermophoresis diffusion coefficient respectively. Furthermore, χ, α_m, $R(x)$, F and q_{ry}'' are heat capacity ratio, effective thermal diffusivity, variable reaction rate, Forchheimer inertia factor and radiative heat flux. We introduce the stream function $\Psi(x,y)$ as follows;

$$u=\frac{\partial \Psi(x,y)}{\partial y},\quad v=-\frac{\partial \Psi(x,y)}{\partial x}. \tag{8}$$

It has shown that, using Eqn (8), Eqn (1) is automatically satisfied and therefore Eqns (2) - (4) become;

$$\frac{\partial}{\partial y}\left(\mu(T)\frac{\partial \Psi}{\partial y}\right)+\rho_f F\sqrt{K}\,\frac{\partial}{\partial y}\left(\left(\frac{\partial \Psi}{\partial y}\right)^2\right)=\left(1-\varphi_\infty\right)\rho_{f\infty}\beta g_x K\frac{\partial T}{\partial y}-\left(\rho_p-\rho_{f\infty}\right)g_x K\frac{\partial \varphi}{\partial y}, \tag{9}$$

$$\frac{\partial \Psi}{\partial y}\frac{\partial T}{\partial x}-\frac{\partial \Psi}{\partial x}\frac{\partial T}{\partial y}=\alpha_m\frac{\partial^2 T}{\partial y^2}+\chi\left(D_B\frac{\partial \varphi}{\partial y}\frac{\partial T}{\partial y}+\frac{D_T}{T_\infty}\left(\frac{\partial T}{\partial y}\right)^2\right)+\frac{\mu(T)}{\left(\rho c_p\right)_f}\left(\frac{\partial^2 \Psi}{\partial y^2}\right)^2-\frac{1}{\left(\rho c_p\right)_f}\frac{\partial q_{ry}''}{\partial y}, \tag{10}$$

$$\frac{\partial \Psi}{\partial y}\frac{\partial \varphi}{\partial x}-\frac{\partial \Psi}{\partial x}\frac{\partial \varphi}{\partial y}=\epsilon D_B\frac{\partial^2 \varphi}{\partial y^2}+\frac{\epsilon D_T}{T_\infty}\frac{\partial^2 T}{\partial y^2}-R(x)\epsilon\left(\varphi-\varphi_\infty\right). \tag{11}$$

On the other hand, Rosseland diffusion approximation provides a quantitatively radiative heat flux of the optically, radiative fluid on the boundary layer flow and is approximated as [34];

$$q_{ry}^{''} = -\frac{4\sigma^*}{3k^*}\frac{\partial T^4}{\partial y}. \tag{12}$$

Assuming that the temperature differences within the nanofluid flow are sufficiently small, as such T^4 may be expressed as a linear function of temperature T and expanding T^4 in Taylor's series about T_∞ and neglecting higher order terms we therefore get;

$$T^4 \approx T_\infty^4 + (T-T_\infty)4T_\infty^3 + o(T-T_\infty)^2 ..... = 4T_\infty^3 T - 3T_\infty^3. \tag{13}$$

Hence, using Eqn (13), Eqn (12) becomes;

$$q_{ry}^{''} = \frac{-4\sigma^*}{3k^*}\frac{\partial T^4}{\partial y} = \frac{-4\sigma^*}{3k^*}\frac{\partial}{\partial y}\left(4T_\infty^3 T - 3T_\infty^4\right) = \frac{-16\sigma^* T_\infty^3}{3k^*}\frac{\partial T}{\partial y}, \tag{14}$$

given that, k^* and σ^* are the Rosseland mean absorption coefficient and Stefan-Boltzmann constant, respectively. In this study, the chemical reaction rate $R(x)$ is modelled as a function of x, and therefore its expression is given as;

$$R(x) = \frac{bR_0}{x}, \tag{15}$$

where, R_0 is a constant chemical reaction rate and b is the reference length along the flow. For the present base fluid, following [31], the dynamic viscosity of the base fluid is considered in the following form:

$$\mu_f(T) = \frac{\mu_\infty}{1+\gamma(T-T_\infty)} = \frac{1}{a(T-T_e)}, \tag{16}$$

where μ_∞ is a dynamic viscosity of the ambient base fluid; γ is a constant value, it implies that when $\gamma = 0$, the dynamic viscosity of the base fluid flow remains constant throughout the system. Apart from that, a and T_e are constants, given by;

$$a = \frac{\gamma}{\mu_\infty},\ T_e - T_\infty = -\frac{1}{\gamma}. \tag{17}$$

Following the lines of [18], we introduced the following dimensionless variables;

$$\eta = \frac{y}{x}Ra_x^{1/2},\ \Psi(x,y) = \alpha_m Ra_x^{1/2} f(\xi,\eta),\ \theta(\xi,\eta) = \frac{T-T_\infty}{T_w-T_\infty},\ C(\xi,\eta) = \frac{\varphi-\varphi_\infty}{\varphi_w-\varphi_\infty},$$
$$\theta_e = \frac{T_e-T_\infty}{T_w-T_\infty},\ \xi = \frac{Pe_x}{Ra_x}. \tag{18}$$

Given that $Pe = \frac{U_\infty x}{\alpha_m}$, $Ra_x = (1-\varphi_\infty)\rho_{f\infty} g_x \beta K (T_w - T_\infty) x/\mu_\infty \alpha_m$, $U_\infty = c\,x^m$ and $g_x = g\cos\left(\frac{\Omega}{2}\right)$ are local Peclet number, local Rayleigh number, potential flow velocity outside a boundary layer and acceleration due to gravity component along x-axis. Moreover, m is related to the angle of a wedge under the expression given by $m = \frac{\Omega/2}{\pi-\Omega/2}$. It implies that, if $m = 0, 1/3, 1/2$ and 1, correspond to a uniform free stream flowing along a vertical plate, a free stream flowing over a $\Omega = 90°$ wedge, a free stream flowing over a $\Omega = 120°$ wedge and a stagnation flow to a vertical wall, $\Omega = 180°$, respectively.
Substituting the Eqns (14)-(18) in Eqns (9)-(11) we get the following dimensionless non-similar boundary layer equations that governed the flow system of nanofluid within the porous medium over a permeable vertical wedge:

$$f''' + \left(\frac{1}{\theta_e-\theta}\right)f'\theta' + 2\lambda\left(\frac{\theta_e-\theta}{\theta_e}\right)f'f'' - \left(\frac{\theta_e-\theta}{\theta_e}\right)\theta' + N_r\left(\frac{\theta_e-\theta}{\theta_e}\right)C' = 0, \tag{19}$$

$$\theta''\left(1+\frac{4}{3\sigma}\right) + \frac{1}{2}f\theta' + N_b C'\theta' + N_t(\theta')^2 + \left(\frac{\theta_e}{\theta_e-\theta}\right)Br(f'')^2 = m\xi\left(f'\frac{\partial\theta}{\partial\xi} - \theta'\frac{\partial f}{\partial\xi}\right), \tag{20}$$

$$C'' + \frac{1}{2}Lef C' + \frac{N_t}{N_b}\theta'' - \delta LeC = Lem\xi\left(f'\frac{\partial C}{\partial\xi} - C'\frac{\partial f}{\partial\xi}\right). \tag{21}$$

Subjected to the following boundary conditions;

$$\eta=0,\ \ f(\xi,0)+2m\xi\frac{\partial f}{\partial \xi}(\xi,0)=S,\ \ \theta(\xi,0)=1,\ \ C(\xi,0)=1,$$
$$\eta\to\infty, f^{'}(\xi,\infty)=\xi,\ \ \theta(\xi,\infty)=C(\xi,\infty)=0, \quad (22)$$

where, primes represent the derivatives with respect to η and $S=-2V_w x/\alpha_m Ra_x^{1/2}=-2V_0 x/\alpha_m Ra_x^{1/2}$ is the suction or injection parameter. Furthermore, S is considered to be either suction or injection parameter if $S>0$ $(i.e, V_0<0)$ and $S<0$ $(i.e, V_0>0)$, respectively. In the transformation process, the following parameters are emerged;

$$\begin{cases} \lambda=\frac{F\sqrt{K}}{\nu_\infty}\left(\frac{(1-\varphi_\infty)\rho_{f\infty}g_x K\beta(T_w-T_\infty)}{\mu_\infty}\right), \\ N_t=\frac{\epsilon(\rho c_p)_p}{(\rho c_p)_f}\frac{D_T}{T_\infty}\frac{(T_w-T_\infty)}{\alpha_m}, Le=\frac{\alpha_m}{\epsilon D_B}, \\ N_r=\frac{(\rho_p-\rho_{f\infty})(\varphi_w-\varphi_\infty)}{\rho_{f\infty}(1-\varphi_\infty)(T_w-T_\infty)\beta}, N_b=\frac{\epsilon(\rho c_p)_p}{(\rho c_p)_f}\frac{D_B}{\alpha_m}(\varphi_w-\varphi_\infty),\ \ \sigma=\frac{kk^*}{4\sigma^* T_\infty^3}, \\ Br=\frac{\mu_\infty}{k(T_w-T_\infty)}\left(\frac{(1-\varphi_\infty)\rho_{f\infty}g_x\beta K(T_w-T_\infty)}{\mu_\infty}\right)^2, \\ \delta=\frac{b\epsilon R_0\mu_\infty}{(1-\varphi_\infty)\rho_{f\infty}g_x\beta K(T_w-T_\infty)}, \end{cases} \quad (23)$$

where, B_r is the modified Brinkmann number, N_t is a thermophoresis parameter, N_r is a buoyancy parameter, N_b is the brownian motion parameter, m is the wedge angle parameter, λ is the modified inertia parameter, δ is the reaction rate parameter, σ is the radiation parameter, k is a thermal conductivity, ξ is the parameter representing the forced flow effect on natural convection flow and Le is the Lewis number. Following the lines of [13], it has showned that θ_e is determined by the viscosity/temperature characteristics of the base fluid and the operating temperature difference is $\Delta T=T_w-T_\infty$ or $\theta_e=-1/\gamma(T_w-T_\infty)$. Apart from that, it is also shown that, if θ_e is small then either the base fluid viscosity changes with temperature difference or the temperature difference is high. It may be noted that for assisting flow θ_e is negative for liquids and positive for gases [31]. Furthermore, it is worth to note that, the chemical reaction is of constructive type if $\delta<0$, destructive type if $\delta>0$ and no reaction type for $\delta=0$. In this study, we classified ξ into three cases: the first case for $\xi=0$ corresponds to pure natural convection, the second case which is known as a limiting case for $\xi=1$ corresponds to pure forced convection flow, while the third case for $\xi=(0-1)$ corresponds to the existence of both effects in the flow. Therefore, in this study both effects within the flow are analyzed in detail.

The quantities of physical interest on the surface of a vertical heated wedge are local Nusselt number Nu_x and local Sherwood number Sh_x , which are defined as follows;

$$Nu_x=\frac{h_w x}{k_m}=\frac{q_w^{''}x}{k_m(T_w-T_\infty)};\ \ q_w^{''}=-k\frac{\partial T}{\partial y}+q_{ry}^{''}, \quad (24)$$

$$Sh_x=\frac{h_m x}{D}=\frac{q_m^{''}x}{D(\varphi_w-\varphi_\infty)}=-\frac{x\frac{\partial\varphi}{\partial y}}{(\varphi_w-\varphi_\infty)}, \quad (25)$$

where $q_w^{''}, q_m^{''}, h_w$ and h_m are heat transfer rate, mass transfer rate, heat transfer coefficient and mass transfer coefficient at the slant surface of a wedge respectively. Furthermore, using Eqn (18), the new expressions of reduced Nusselt number and reduced Sherwood number are obtained as follows;

$$Nu_x=-Ra_x^{\frac{1}{2}}\left(1+\frac{4}{3\sigma}\right)\left(\theta^{'}(\xi,0)\right),\ \ Sh_x=-Ra_x^{\frac{1}{2}}\left(C^{'}(\xi,0)\right), \quad (26)$$

$$Nu_r=\frac{Nu_x}{Ra^{\frac{1}{2}}{}_x}=-\left(1+\frac{4}{3\sigma}\right)\theta^{'}(\xi,0),\ \ Sh_r=\frac{Sh_x}{Ra^{\frac{1}{2}}{}_x}=-C^{'}(\xi,0). \quad (27)$$

3. Local non-similarity method.

This section describes a local non-similarity technique initiated by [33] and it has been applied to solve several non-similarity boundary layer problems. Using a non-similarity method, the local non-similarity solutions are computed by solving Eqns (19)-(21) together with an auxiliary system of equations. An auxiliary system of equations which support an initial partial differential equations (Eqns (19)-(21)) during computations are formed by differentiating Eqns (19) -(21) with respect to ξ. Apart from that, the second level of truncation for auxiliary systems is created by

neglecting all terms involving the product of ξ and $\frac{\partial^2}{\partial\xi^2}()$, that means $\xi\frac{\partial^2}{\partial\xi^2}()$ be equal to zero . For the higher level of truncations, in this case, the second levels of truncation, the following expressions are introduced:

$$f_1=\frac{\partial f}{\partial\xi},\ f_1^{'}=\frac{\partial f^{'}}{\partial\xi},\ f_1^{''}=\frac{\partial f^{''}}{\partial\xi},\ f_2=\frac{\partial f_1}{\partial\xi},\ \theta_1=\frac{\partial\theta}{\partial\xi},\ \theta_1^{'}=\frac{\partial\theta^{'}}{\partial\xi},\ C_1=\frac{\partial C}{\partial\xi},\ C_1^{'}=\frac{\partial C^{'}}{\partial\xi}. \tag{28}$$

Therefore, the systems of equations up to the second level of truncations obtained are as follows;

$$f^{''}+\left(\frac{1}{\theta_e-\theta}\right)f^{'}\theta^{'}+2\lambda\left(\frac{\theta_e-\theta}{\theta_e}\right)f^{'}f^{''}-\left(\frac{\theta_e-\theta}{\theta_e}\right)\theta^{'}+N_r\left(\frac{\theta_e-\theta}{\theta_e}\right)C^{'}=0, \tag{29}$$

$$\theta^{''}\left(1+\frac{4}{3\sigma}\right)+\frac{1}{2}f\theta^{'}+N_bC^{'}\theta^{'}+N_t\left(\theta^{'}\right)^2+\left(\frac{\theta_e}{\theta_e-\theta}\right)Br\left(f^{''}\right)^2=m\xi\left(f^{'}\theta_1-\theta^{'}f_1\right), \tag{30}$$

$$C^{''}+\frac{1}{2}LefC^{'}+\frac{N_t}{N_b}\theta^{''}-\delta LeC=Lem\xi\left(f^{'}C_1-C^{'}f_1\right), \tag{31}$$

$$f_1^{''}\left(1+2\lambda f^{'}-\frac{2\lambda}{\theta_e}\theta f^{'}\right)+\frac{1}{(\theta_e-\theta)}\left(f_1^{'}\theta^{'}+f^{'}\theta_1^{'}\right)+\frac{\theta_1f^{'}\theta^{'}}{(\theta_e-\theta)^2}+2\lambda f_1^{'}f^{''}-\theta_1^{'}$$
$$-\frac{2\lambda}{\theta_e}\left(\theta_1f^{'}f^{''}+\theta f_1^{'}f^{''}\right)+\frac{1}{\theta_e}\left(\theta_1\theta^{'}+\theta\theta_1^{'}\right)+N_rC_1^{'}-\frac{N_r}{\theta_e}\left(\theta_1C^{'}+\theta C_1^{'}\right)=0, \tag{32}$$

$$\theta_1^{''}\left(1+\frac{4}{3\sigma}\right)+\frac{1}{2}\left(f_1\theta^{'}+f\theta_1^{'}\right)+N_b\left(C_1^{'}\theta^{'}+C^{'}\theta_1^{'}\right)+2N_t\theta^{'}\theta_1^{'}+\frac{Br\theta_e}{(\theta_e-\theta)^2}\theta_1\left(f^{''}\right)^2$$
$$+\frac{2Br\theta_e}{(\theta_e-\theta)}f^{''}f_1^{''}=m\left(f^{'}\theta_1-\theta^{'}f_1+\xi\left(f_1^{'}\theta_1-\theta_1^{'}f_1\right)\right), \tag{33}$$

$$C_1^{''}+\frac{1}{2}Le\left(f_1C^{'}+fC_1^{'}\right)+\frac{N_t}{N_b}\theta_1^{''}-\delta LeC_1=mLe\left(f^{'}C_1-C^{'}f_1+\xi\left(f_1^{'}C_1-C_1^{'}f_1\right)\right). \tag{34}$$

In the analysis, the terms involved on the right hand side of Eqns (30)-(31) are kept in the system, while those terms obtained through differentiating the original system of equations with respect to ξ, for instance, $\frac{\partial f_1}{\partial\xi}$, $\frac{\partial\theta_1}{\partial\xi}$ and $\frac{\partial C_1}{\partial\xi}$ on the right hand side of an auxiliary system of equations (Eqns (33)-(34)) are neglected. Hence, the boundary conditions to be satisfied the Eqns (29)-(34) are given as;

$$\begin{cases} f(\xi,0)+2m\xi f_1(\xi,0)=S,\ \ \theta(\xi,0)=1,\ \ C(\xi,0)=1,\\ f^{'}(\xi,\infty)=\xi,\ \ \theta(\xi,\infty)=C(\xi,\infty)=0\\ f_1(\xi,0)=0,\ \ \theta_1(\xi,0)=0,\ \ C_1(\xi,0)=0,\\ f_1^{'}(\xi,\infty)=1,\ \ \theta_1(\xi,\infty)=0,\ \ C_1(\xi,\infty)=0. \end{cases} \tag{35}$$

Using [33] approach, Eqns (29)-(35) can be considered as a system of non-linear ordinary differential equations for the unknown functions, f,θ,C,f_1,θ_1 and C_1 together with ξ as a parameter, like other parameters involved in the system. Further, the local non-similarity solutions of Eqns (29)-(34) together with their boundary conditions, Eqn (35) can be evaluated by converting the problem into a system of twelve first order equations with twelve boundary conditions as indicated in Eqn (35).

4. Numerical solutions

The non-linear ordinary differential Eqns (29)-(34) which are formed by using local non-similarity method together with their boundary condition, Eqn (35), have been solved numerically by employing the fourth order Runge-Kutta scheme, alongside with shooting method. At any downstream location a parameter ξ , is regarded to be constant. Apart from that, the system of equations is therefore evaluated as if they are non-linear ordinary differential equations. In the analysis, the main interest is to obtain solutions for the functions, f,θ and C and their derivatives with respect to η of the system. The proper guessing of $f^{'}(\xi,0)$, $\theta^{'}(\xi,0)$, $C^{'}(\xi,0)$, $f_1^{'}(\xi,0)$, $\theta_1^{'}(\xi,0)$ and $C_1^{'}(\xi,0)$ was done with the help of shooting technique. Also, the step size of $\Delta\eta=0.001$ and the accuracy of 10^{-8} as the criterion of convergence were used to get the local non-similarity solutions numerically. The computations have been done using various parameter values. The following parameters were considered in the analysis, namely, modified Brinkmann number B_r, thermophoresis parameter N_t, buoyancy parameter N_r, brownian motion parameter N_b, the wedge angle parameter m, the modified inertia parameter λ, the reaction rate parameter δ, the radiation parameter σ, the parameter representing the forced flow effect on natural convection flow ξ and Lewis number Le. The dimensionless velocity, temperature, nanoparticle volume fraction, reduced Nusselt number and reduced Sherwood number profiles were presented in graphical forms. In the following section, the effects of the parameters governing the problem are explained in detail.

5. Results and Discussion

In our present investigation, we have solved numerically and analyzed the theoretical solutions of dimensionless non-linear ordinary differential equations obtained through the use of local non-similarity method with second level of truncation. The problems formed, namely, the non-linear ordinary differential equations with initial boundary conditions, rate of heat and mass transfer from a permeable vertical wedge embedded in the porous medium are solved numerically by the use of fourth order Runge-Kutta with shooting method. Numerical analysis are carried out for $\theta_e \leq -2$, $0.001 \leq \lambda \leq 0.7$, $\sigma \geq 1$, $0.1 \leq N_r \leq 0.5$, $0.1 \leq N_b \leq 5$, $0.1 \leq N_t \leq 3$, $Le \geq 1$, $0.1 \leq Br \leq 3$, $\delta \geq 1$, $-3 \leq S \leq 3$, $0 \leq m \leq 1$ and $0 \leq \xi \leq 1$. The effects of various parameters on the dimensionless velocity, temperature, nanoparticle volume fraction, reduced Nusselt number and reduced Sherwood number in the boundary layer flow have shown in graphical form. A detail elaboration is provided for every parameter involved in the simulation. Also, we have observed that the results of present research using the local non-similarity method with the absence of modified Brinkmann number in the boundary layer flow, $Br = 0$, thermal radiation, $\sigma \to \infty$, constant dynamic viscosity, $\theta_e \to -\infty$, no chemical reaction, $\delta = 0$ and no inertia effect in the flow, $\lambda = 0$ are in very good agreement with those found in [18].

Figs. 2, 3 and 4 display results for dimensionless velocity, temperature and nanoparticle volume fraction profiles over a vertical wedge embedded in a porous medium. In Figs 2, 3 and 4, we note that as θ_e decreases, the velocity profiles decrease, whereas both temperature and nanoparticle profiles in the boundary layer increase, respectively. Here, we noted that, the decrease of dimensionless velocity of nanofluid on the boundary layer is caused by the decrease of temperature gradient between a wedge and the ambient temperature of the flow. Figs. 5, 6 and 7 indicate that, as λ increases, the dimensionless velocity and temperature decrease and nanoparticle volume fraction profiles increase. Here we observed that, the decrease of dimensionless velocity and temperature in the boundary layer flow is due to the increase of form drag on the porous medium to the flow.

The numerical solutions of dimensionless velocity, temperature and nanoparticle volume fraction are displayed in Figs. 8, 9 and 10 for different radiation parameter σ. It is found from Figs 8 and 9 that, as σ increases, the velocity and temperature profiles decrease in the boundary layer. This indicates that, the σ tends to retard nanofluid velocity and decrease temperature in the porous medium, whereas in Fig. 10, as the σ increases, nanoparticle volume fraction increases.

In Figs 11, 12 and 13, the dimensionless velocity, temperature and nanoparticle volume fraction profiles are plotted against similarity variable η for different values of Brinkmann number, Br. It is observed that when the values of Br increase, the dimensionless velocity and temperature profiles increase in the boundary layer, whereas the nanoparticle volume fraction profiles decrease as shown in Fig. 13. This effect is caused by the increment of heat generated within a boundary layer due to different relative velocities of the flow. Figs. 14, 15 and 16 demonstrate the effects of reaction parameter, δ on dimensionless velocity, temperature and nanoparticle volume fraction profiles with similarity variable, η. It is noted that, the dimensionless velocity increases near a wedge surface and decreases across similarity variable, η to free stream velocity, whereas, temperature and nanoparticle volume fraction decrease as δ values increase in the boundary layer.

Figs. 17, 18 and 19 show the dimensionless velocity, temperature and nanoparticle volume fraction profiles for different values of suction/injection parameter, S. It is observed that, both profiles decrease as suction parameter increase and both profiles in the boundary layer flow increase as injection parameter decrease. Furthermore, it has noted that, the decrease of injection parameter enhances the boundary layer thickness of both profiles within a flow. Also, we observed that, the suction effect retards the motion of the nanofluid when imposed on a vertical wedge as presented in Fig. 17.

Figs. 20, 21 and 22 represent the dimensionless velocity, temperature and nanoparticle volume fraction profiles for different thermophoresis parameter values, N_t. We observed that both profiles of velocity, temperature and nanoparticle volume fraction increase with the increase of thermophoresis parameter values in the boundary layer.

In Figs. 23, 24 and 25, the dimensionless velocity, temperature and nanoparticle volume fraction plotted against the similarity variable, η for different values of buoyancy ratio parameter, N_r. It indicates that both velocity and temperature decrease with increase in buoyancy ratio parameter values, whilst the nanoparticle volume fraction increases as the buoyancy ratio parameter increases. Furthermore, in Figs. 26, 27 and 28, the dimensionless velocity, temperature and nanoparticle volume fraction plotted against the similarity variable, η for different values of brownian motion parameter, N_b. It indicates that as the brownian motion parameter increass, dimensionless velocity increases near a surface of the wedge and then decreases on increasing of η to approach free stream value and temperature increases with increase in brownian motion parameter values. Whilst the nanoparticle volume fraction decreases as the brownian motion parameter increases within the boundary layer flow.

Figs. 29, 30 and 31 depict, the dimensionless velocity, temperature and nanoparticle volume fraction for different values of Lewis number, Le for fixed values of other physical parameters. As the Lewis number increases, the dimensionless velocity profiles increase, however both temperature and nanoparticle volume fraction profiles decrease with increase in Lewis number. In this case, it is observed that, the increase in dimensionless velocity is due to increase of heat diffusion from a wedge to the boundary layer flow. Also, Figs. 32, 33 and 34 show the dimensionless velocity, temperature and nanoparticle volume fraction profiles with varying wedge angle parameter, m. As the wedge angle parameter increases, both velocity and temperature profiles increase with increase in wedge angle parameter, but the nanoparticle volume fraction decreases with increase in wedge angle parameter.

The variation of heat transfer rate, $Nu_x/Ra_x^{1/2}$ and mass transfer rate, $Sh_x/Ra_x^{1/2}$ with ξ are shown in Fig. 35 with varying Brinkmann number, Br. It is found that as Br increases, heat transfer rate decreases, whilst the mass transfer rate increases. This is due to the fact that, increasing of heat in the boundary layer due to viscous dissipation hinders the heat transfer from a wedge to a boundary layer flow. Also, the results show that as the suction parameter increases, both heat and mass transfer increase in the surface of a vertical wedge as presented in Fig. 36

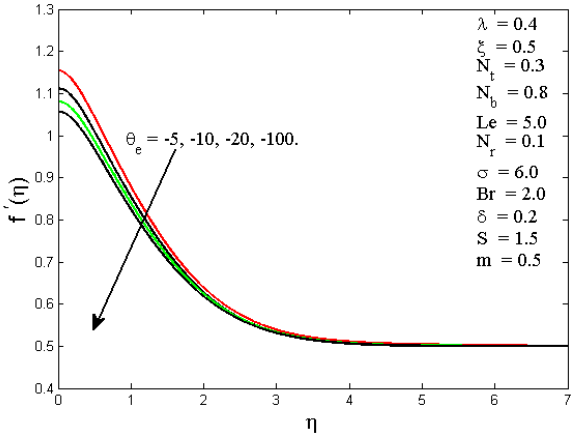

Fig. 2. Effects of variable viscosity parameter, θ_e on velocity profiles.

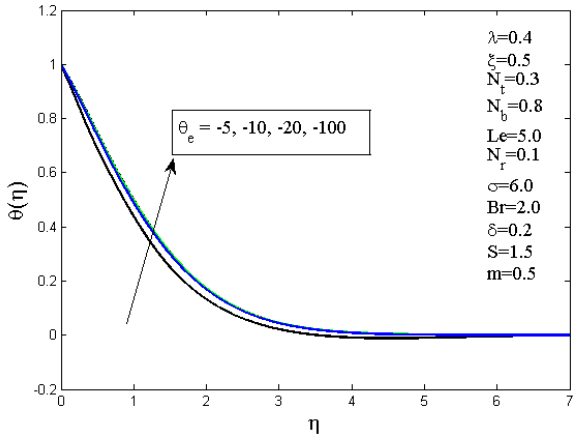

Fig. 3. Effects of variable viscosity parameter, θ_e on temperature profiles.

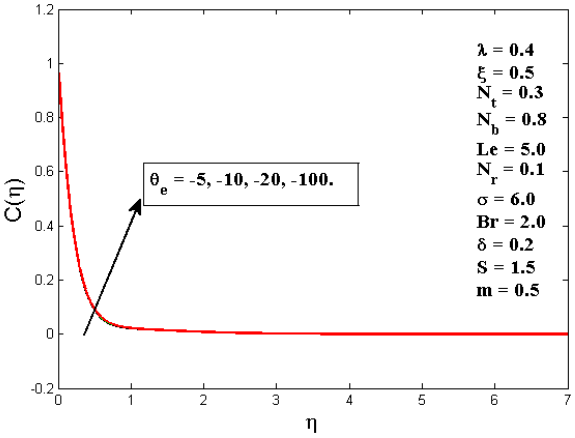

Fig. 4. Effects of variable viscosity parameter, θ_e on nanoparticle volume fraction profiles.

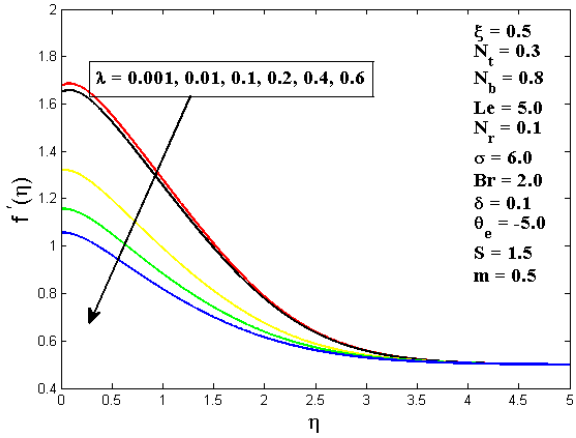

Fig. 5. Effects of modified inertia parameter, λ on velocity profiles.

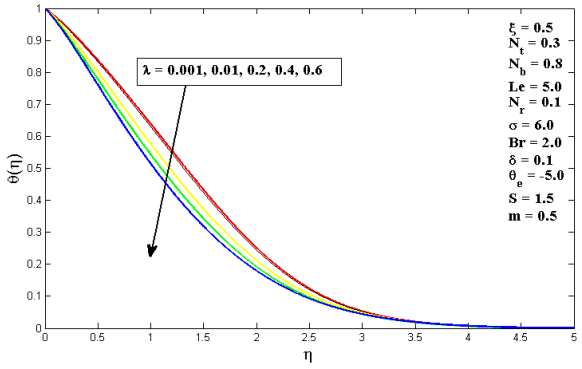

Fig. 6. Effects of modified inertia parameter, λ on temperature profiles.

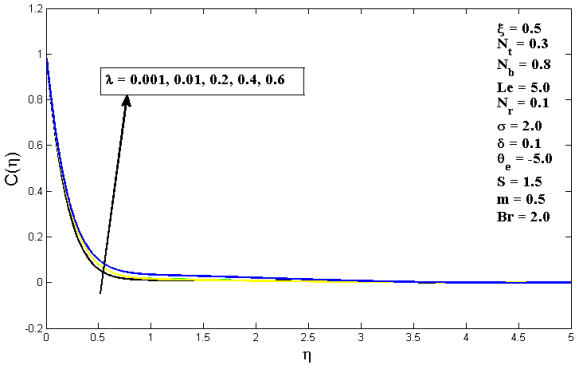

Fig. 7. Effects of modified inertia parameter, λ on nanoparticle volume fraction profiles.

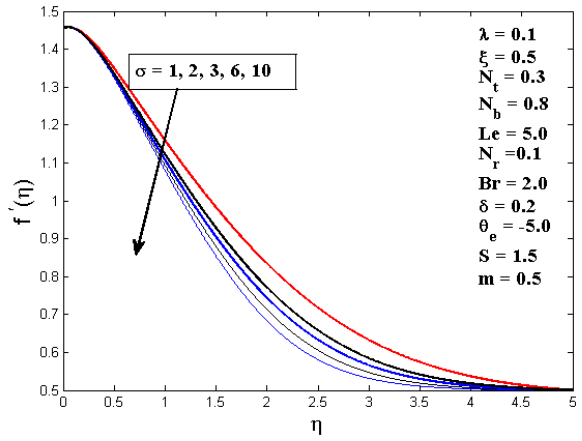

Fig. 8. Effects of radiation parameter, σ on velocity profiles.

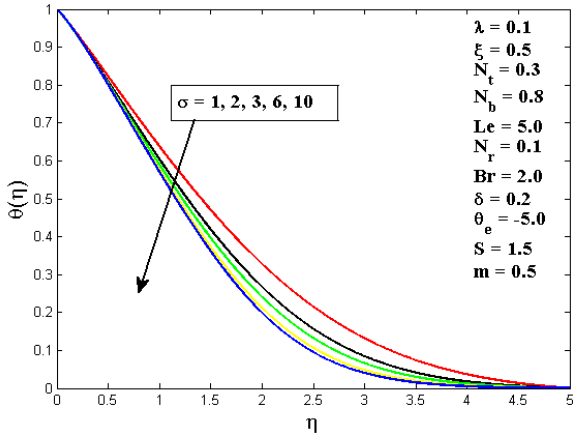

Fig. 9. Effects of radiation parameter, σ on temperature profiles.

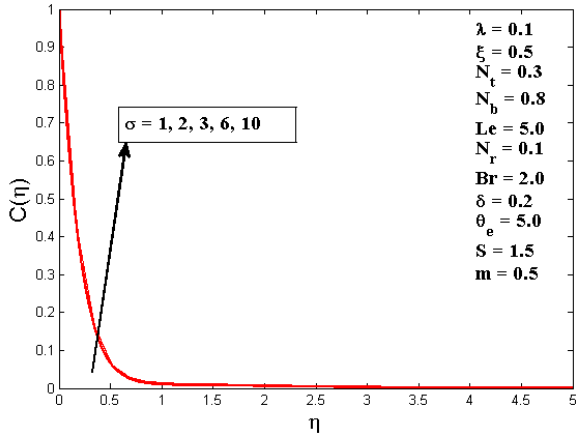

Fig. 10. Effects of radiation parameter, σ on nanoparticle volume fraction profiles.

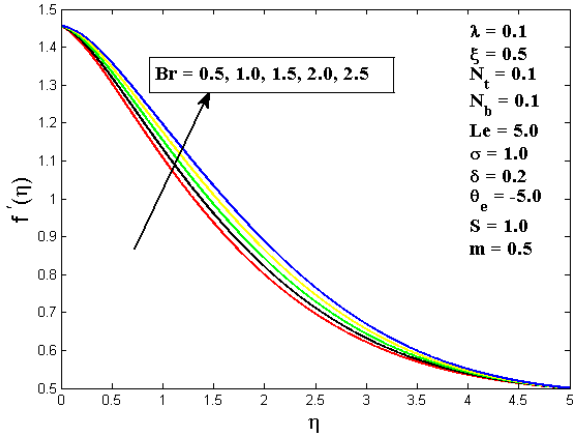

Fig. 11. Effects of Brinkmann number, Br on velocity profiles.

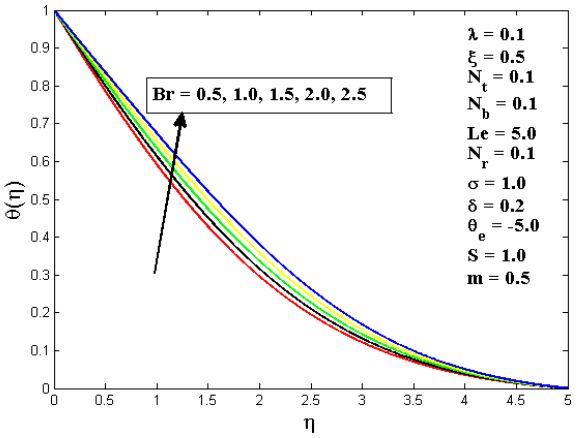

Fig. 12. Effects of Brinkmann number, Br on temperature profiles.

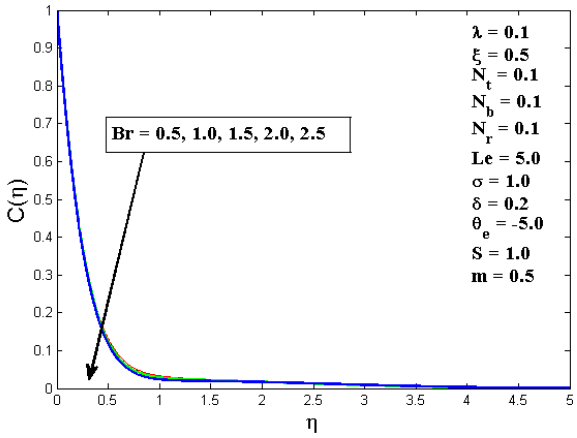

Fig. 13. Effects of Brinkmann number, Br on nanoparticle volume fraction profiles.

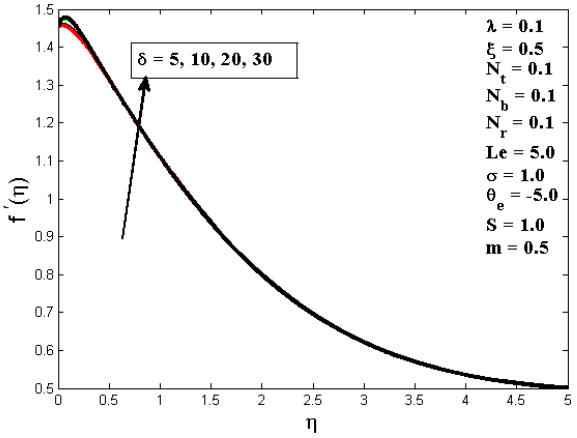

Fig. 14. Effects of reaction rate parameter, δ on velocity profiles.

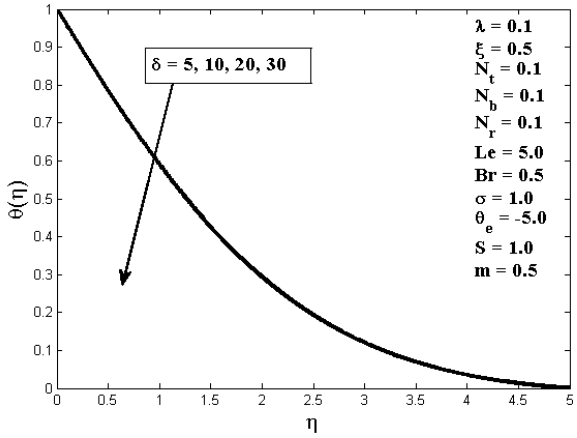

Fig. 15. Effects of reaction rate parameter, δ on temperature profiles.

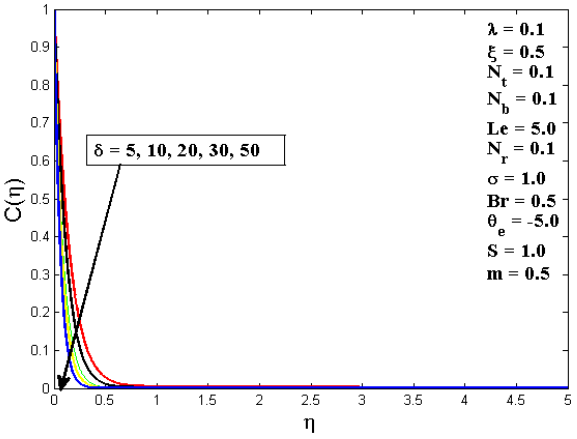

Fig. 16. Effects of reaction rate parameter, δ on nanoparticle volume fraction profiles.

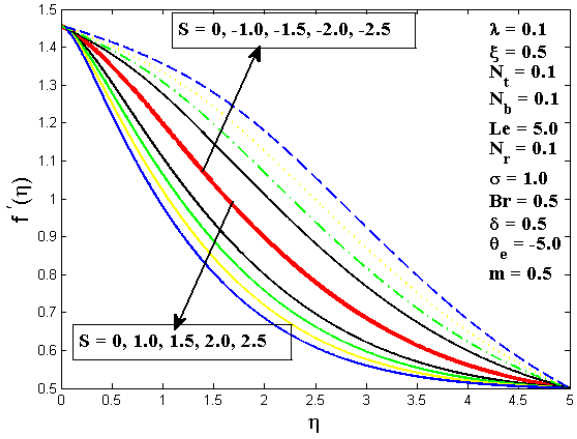

Fig. 17. Effects of suction/injection parameter, S on velocity profiles.

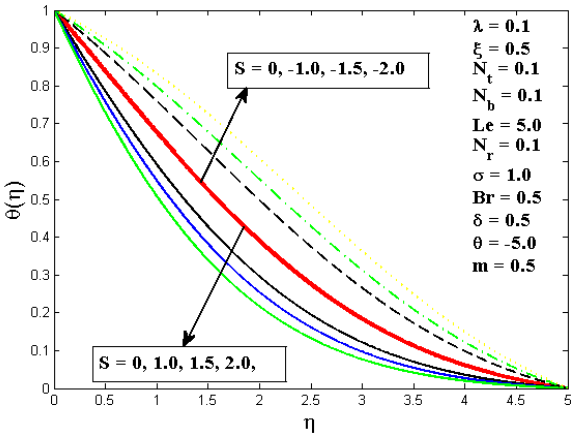

Fig. 18. Effects of suction/injection parameter, S on temperature profiles.

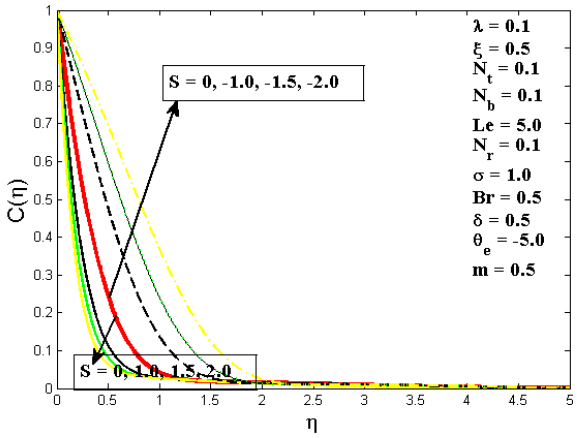

Fig. 19. Effects of suction/injection parameter, S on nanoparticle volume fraction profiles.

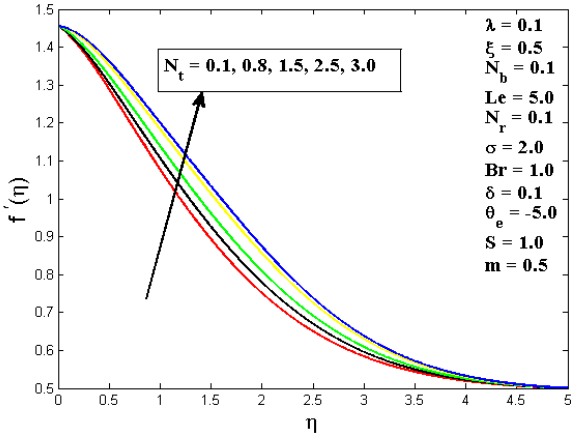

Fig. 20. Effects of thermophoresis parameter, N_t on velocity profiles.

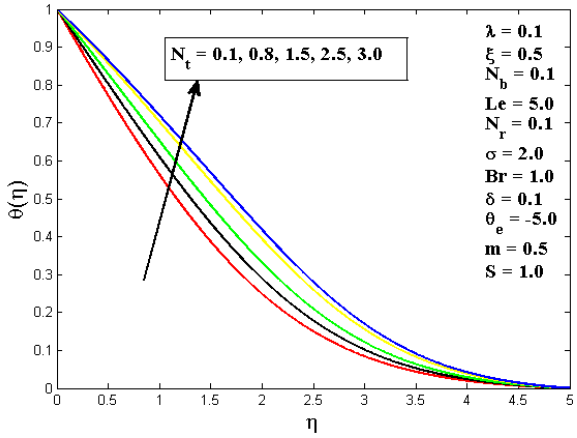

Fig. 21. Effects of thermophoresis parameter, N_t on temperature profiles.

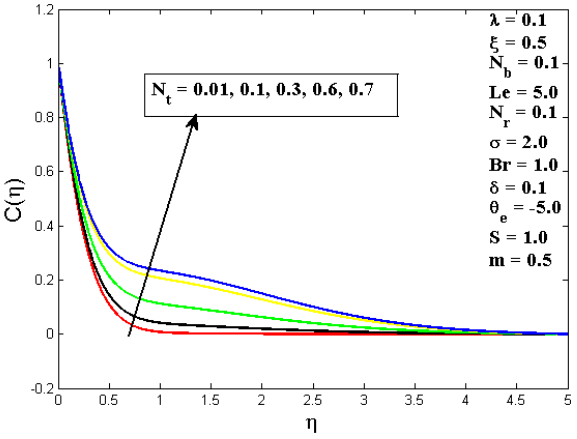

Fig. 22. Effects of thermophoresis parameter, N_t on nanoparticle volume fraction profiles.

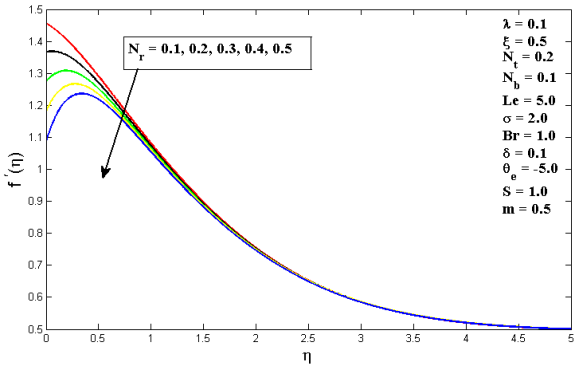

Fig. 23. Effects of buoyancy ratio parameter, N_r on velocity profiles.

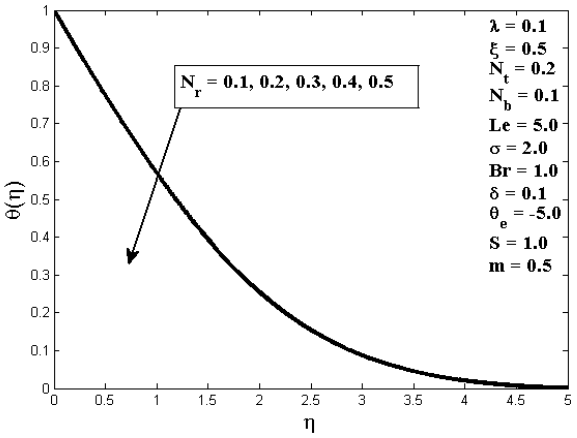

Fig. 24. Effects of buoyancy ratio parameter, N_r on temperature profiles.

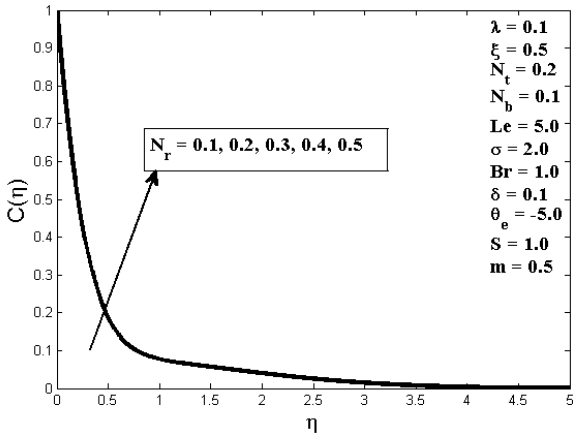

Fig. 25. Effects of buoyancy ratio parameter, N_r on nanoparticle volume fraction profiles.

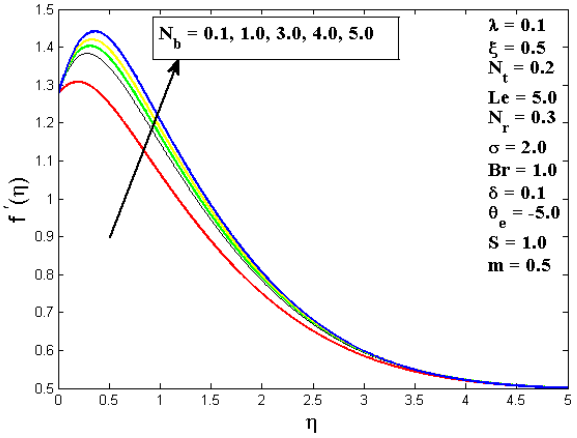

Fig. 26. Effects of brownian motion parameter, N_b on velocity profiles.

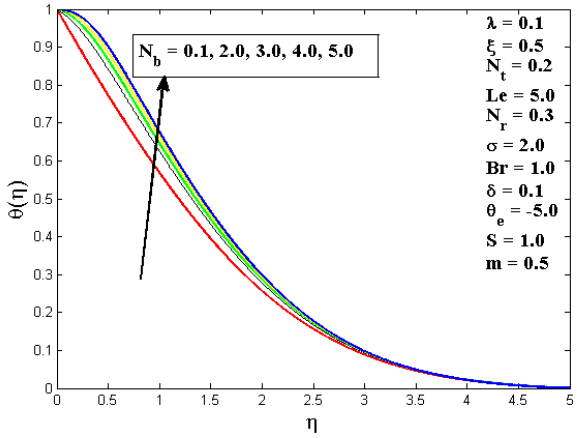

Fig. 27. Effects of brownian motion parameter, N_b on temperature profiles.

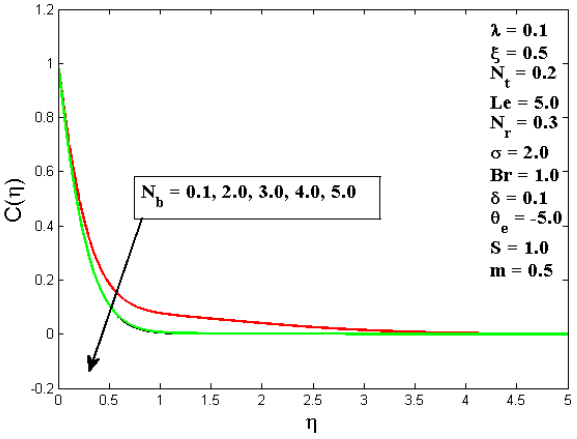

Fig. 28. Effects of brownian motion parameter, N_b on nanoparticle volume fraction profiles.

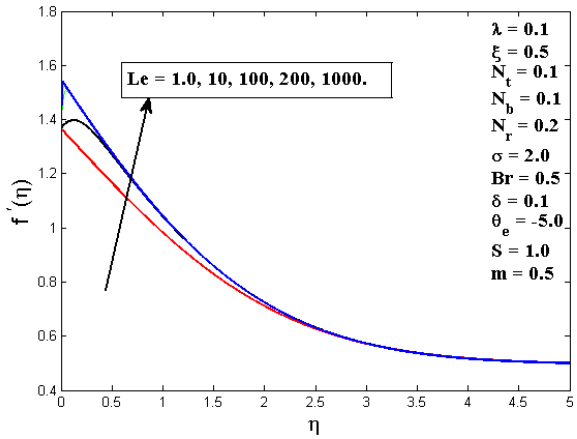

Fig. 29. Effects of Lewis number, Le on velocity profiles.

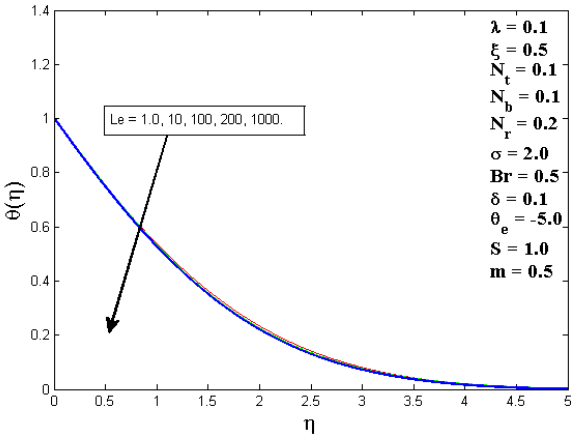

Fig. 30. Effects of Lewis number, Le on temperature profiles.

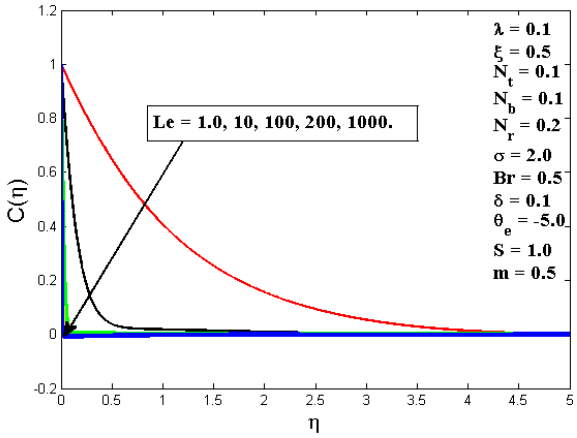

Fig. 31. Effects of Lewis number, Le on nanoparticle volume fraction profiles.

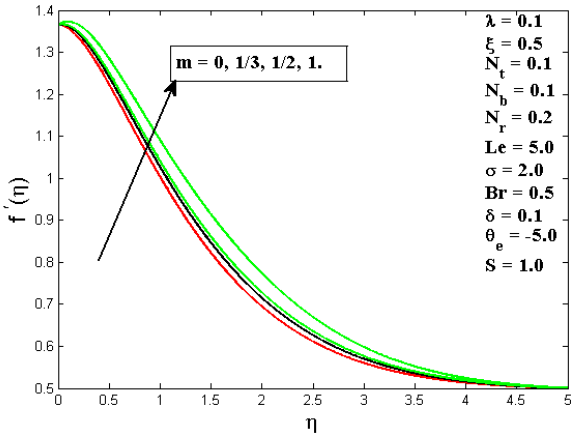

Fig. 32. Effects of wedge angle parameter, m on velocity profiles.

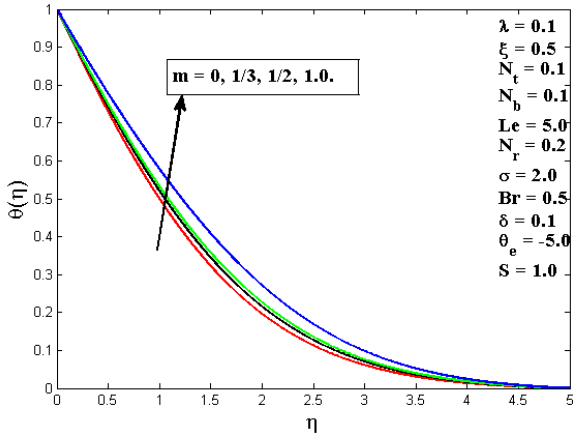

Fig. 33. Effects of wedge angle parameter, m on temperature profiles.

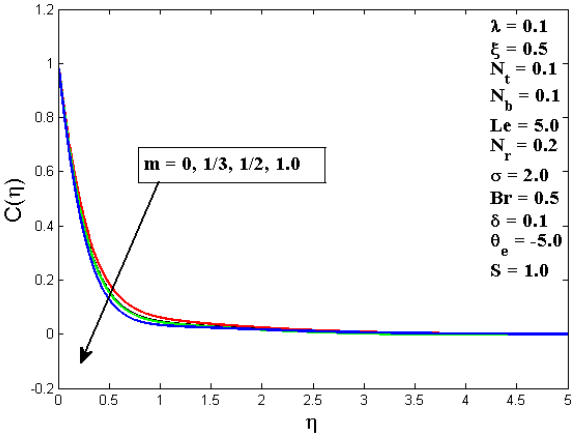

Fig. 34. Effects of wedge angle parameter, m on nanoparticle volume fraction profiles.

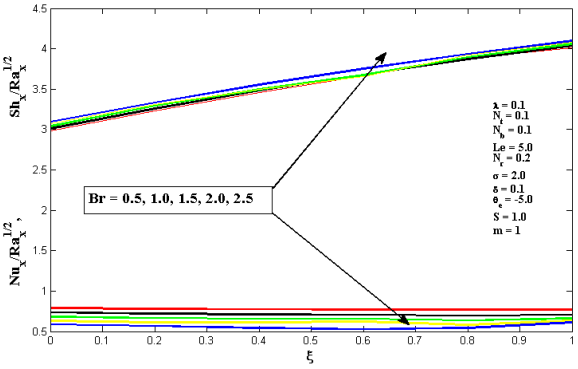

Fig. 35. Effects of Brinkmann number, Br on heat transfer rate (Nusselt number) and mass transfer rate (Sherwood number) with different non-similarity parameter.

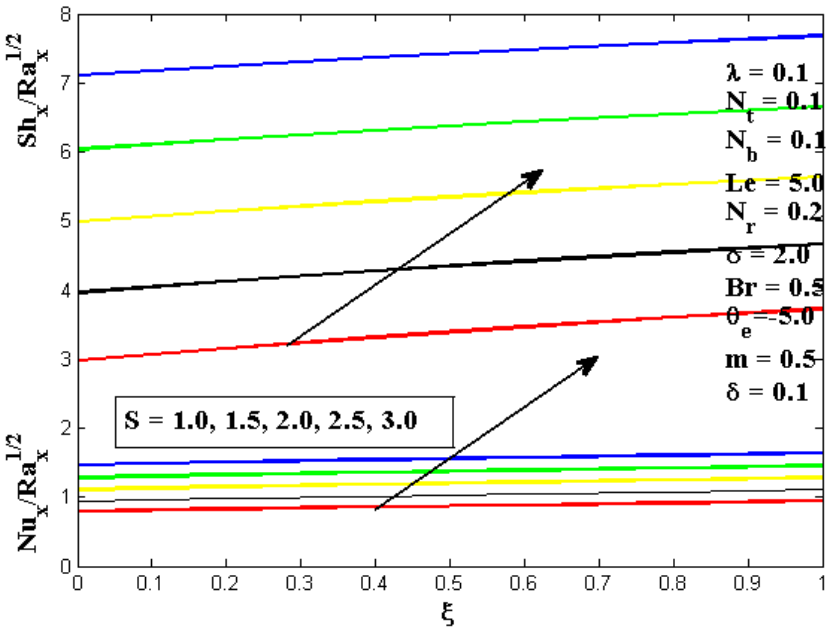

Fig. 36. Effects of suction parameter, S on heat transfer rate (Nusselt number) and mass transfer rate (Sherwood number) with different non-similarity parameter.

6. Conclusion

In the present study, we have investigated the effects of variable viscosity of nanofluid flow over a vertical permeable wedge embedded in saturated porous medium with chemical reaction and heat radiation. We have extended the previous study by taking into consideration the effects of injection and suction together with forced flow effect on the permeable vertical wedge surface. Here, the effects of various thermophysical parameters arise from the governing system of equations on the flow of nanofluid over a permeable vertical wedge embedded in a porous medium have discussed in detail. The results of this study can be summarized as follows;

- The nanoparticle volume fraction thickness decreases with the increase of reaction rate parameter and Lewis number within the boundary layer.
- The momentum boundary layer, thermal boundary layer and nanoparticle volume fraction layer thicknesses increase with the decrease of injection parameter.
- The rate of heat transfer (reduced Nusselt number) increases as the radiation parameter increases. This indicates that, thermal radiation plays an important role in contributing significant heat to the total heat transfer rate from a wedge.
- The rate of heat transfer (reduced Nusselt number) and rate of mass transfer (reduced Sherwood number) are enhanced on the surface of a wedge, by increasing the suction parameter on the surface.
- The rate of heat transfer (reduced Nusselt number) at the surface of a wedge decreases with the increases in the Brinkmann number, whilst the mass transfer rate increases as the Brinkmann number increases.
- The reduced Nusselt number at the surface of a wedge increases as inertia parameter which is arise from Forchheimer term increases, while the reduced Sherwood number decreases as the inertia parameter increases.
- The heat transfer rate and mass transfer rate increase with the increase of variable viscosity parameter.
- Both reduced Nusselt and Sherwood numbers are enhanced from the surface of a wedge by increasing the forced flow effect to the natural convection flow in boundary layer.
- With the increase of wedge angle parameter, the reduced Nusselt number decreases, while the reduced Sherwood number increases at the surface of a wedge.

References

[1] T. L. Olaseni, R. A. Olafenwa, Analytical Solution of a Steady Non-Reacting Laminar Fluid Flow in a Chemical Filled With Saturated Porous Media with Two Distinct Horizontal Impermeable Wall Conditions, Journal of Natural Sciences Research. 2(2012).

[2] K. Vafai, Handbook of porous media. CRC press Taylor and Francis Group. 2nd ed., New York, 2005.

[3] I. Pop, D. B. Ingham, Convective Heat Transfer-Mathematical and Computational Modeling of viscous fluids and porous media. Oxford OX5 IGB. UK, 2001

[4] M. Q. Al-odat, A. Al-Ghamdi, Numerical investigation of Dufour and Soret effects on unsteady MHD natural convection flow past vertical plate embedded in non-Darcy porous medium, Applied Mathematics and Mechanics (English Edition), 33(2)(2012) 195 - 210.

[5] A. Bejan, A. D. Nield, Convection in porous medium. Springer Science +Business media.inc. 3rd., 2006.

[6] S. P. Anjali Devi, D. Vasantha kumari, Numerical investigation of slip flow effects on unsteady hydromagnetic flow over a stretching surface with thermal radiation, Int. J. Adv. Appl. Math. andMech. 1(4) (2014) 20 - 32.

[7] M. H. Yasin, R. Arifin, Mixed convection boundary layer flow on a vertical surface in a porous medium saturated by a nanofluid with suction or injection, Journal of Mathematics and Statistics, 2(9)(2013) 119 - 128.

[8] S. P. Anjali, A. Julie, Laminar boundary layer flow of nanofluid over a flat plate, Int. J. of Appl. Math and Mech. 7(6)(2011) 52-71.

[9] M. A. Hossain, M. S. Munir, R. S. R. Gorla, Combined Convection from a Vertical Flat Plate with Temperature Dependent Viscosity and Thermal Conductivity, International Journal of Fluid Mechanics Researchl. 29(6)(2002) 725 - 741.

[10] K. R. Deka, S. Sharma, Effects of variable viscosity on mixed convection heat and mass transfer past a wedge with variable temperature, International Journal of Mathematical Archive. 5(5)(2014) 150 - 157.

[11] R. Kandasamy, R. Saravanan, S. K. K. Prabhu, Chemical Reaction on Non-Linear Boundary Layer Flow over a Porous Wedge with Variable Stream Conditions, Chemical Engineering Communications. 197(2010) 522-543.

[12] M. S. Alam, M. Nurul Huda, A new approach for local similarity solutions of an unsteady hydromagnetic free convective heat transfer flow along a permeable flat surface, International Journal of Advances in Applied Mathematics and Mechanics. 1(2)(2013) 39-52.
[13] J. Makungu, E. W. Mureithi, D. Kuznetsov, Free convection flow past an impermeable wedge embedded in nanofluid saturated porous medium with variable viscosity base fluid, Journal of Mathematical and Computational Science. 4(2014) 20-29.
[14] E. W. Mureithi, A Mixed Convection Boundary Layer Flow over a Vertical Wall in a Porous Medium, with Exponentially Varying Fluid Viscosity, Journal of Applied Mathematics and Physics. 2(2014) 795-802.
[15] R. Kandasamy, I. Hashim, Muhaimin, Ruhaila, Effects of variable viscosity, heat and mass transfer on non-linear mixed convection flow over a porous wedge with heat radiation in the presence of homogeneous chemical reaction, ARPN Journal of Engineering and Applied Sciencesl. 2(5)(2007) 44-53.
[16] Muhaimin, R. Kandasamy, I. Hashim, Variable viscosity and thermophoresis effects on Darcy mixed convective heat and mass transfer past a porous wedge in the presence of chemical reaction, Theoret. Appl. Mech. 36(1)(2009) 29-46.
[17] C. H. RamReddy, P. V. S. N Murthy, A. J. Chamkha, A. M. Rashad, Influence of viscous dissipation on free convection in a non-Darcy porous medium saturated with nanofluid in the presence of magnetic field, The open transport phenomena Journal. 5(2013) 20-29.
[18] R. S. S. Gorla, A. J. Chamkha, A. M. Rashad, Mixed convective boundary layer flow over a vertical wedge embedded in a porous medium saturated with a nanofluid: Natural Convection, Nanoscale Research Letter-a SpringerOpen Journal. 6(107)(2011).
[19] N. Pandya, A. K. Shukla, Soret-Dufour and Radiation effect on unsteady MHD flow over an inclined porous plate embedded in porous medium with viscous dissipation, Int. J. Adv. Appl. Math. and Mech. 2(1) (2014) 107 - 119.
[20] A. Noghrehabadi, A. Behseresht, M. Ghalambaz, Natural convection flow of nanofluids over vertical cone embedded in non-Darcy porous media,Journal of thermophysics and heat transfer. 27(2)(2013).
[21] P. Geetha, M. B. K. Moorthy, Variable Viscosity, Chemical Reaction and Thermal Stratification Effects on Mixed Convection Heat and Mass Transfer along a Semi-Infinite Vertical Plate, American Journal of Applied Sciences. 8(6)(2011) 628-634.
[22] A. M. Salem, Coupled heat and mass transfer in Darcy-Forchheimer mixed convection from a vertical flat plate embedded in a fluid-saturated porous medium under the effects of radiation and viscous dissipation, Journal of the Korean Physical Society. 48(3)(2006) 409-413.
[23] S. Das, M. Jana, N. R. Jana, Effects of radiation and viscous dissipation on unsteady free convective flow past a moving vertical porous plate embedded in a porous medium, Communications in Applied Sciences. 1(1)(2013) 59-80.
[24] R. T. Raja, C. N. B. Rao, Effects of Variable Fluid Properties on Free Convection Flows and Heat Transfer at an Isothermal Vertical plate Embedded in a Porous Medium in the presence of Magnetic field and Radiation, International Journal of Advanced Research in Computer Science and Software Engineering. 3(5)(2013) 31-38.
[25] I. L. Animasaun, O. B. Aluko, Analysis on variable fluid viscosity of Non-Darcian flow over a moving vertical plate in a porous medium with suction and viscous dissipation, IOSR Journal of Engineering (IOSRJEN). 4(8)(2014) 18-32.
[26] T. M. N. Eldabe, A. G. Elsaka, A. E. Radwan, A. M. M. Eltaweel, Effects of chemical reaction and heat radiation on the MHD flow of viscoelastic fluid through a porous medium over a horizontal Stretching Flat Plate, Journal of American Science. 6(9)(2010) 126-136.
[27] M. M. Nandeppanavar, M. N. Siddalingappa, Effect of viscous dissipation and thermal radiation on heat transfer over a non-linearly stretching sheet through porous medium, International Journal of Applied Mechanics and Engineering. 18(2)(2013) 461-474.
[28] R. R. Kairi, P. V. S. N. Murthy, C. O. Ng, Effect of viscous dissipation on natural convection in a non-Darcy porous medium saturated with non-Newtonian fluid of variable viscosity, The Open Transport Phenomena Journal. 3(2011) 1-8.
[29] B. Shanker, B. P. Reddy, J. A. Rao, Radiation and mass transfer effects on unsteady MHD free convective fluid flow embedded in a porous medium with heat generation/absorption, Indian Journal of Pure and applied Physics. 48(2010) 157-165.
[30] M. S. Babu, S. P.V. Narayana, T. S. Reddy, D. U. Reddy, Radiation and chemical reaction effects on an unsteady MHD convection flow past a vertical moving porous plate embedded in a porous medium with viscous dissipation, Advances in Applied Science Research. 2(5)(2011) 226-239.
[31] S. M. Abdelgaied, M. R. Eid, Mixed convection flow of Nanofluids over a vertical surface embedded in a porous medium with temperature dependent viscosity, Recent advances in mathematical methods and computational techniques in modern science. 3(2)(2013) 300 - 312.
[32] M. R. Gnaneswara, Heat and mass transfer effects on unsteady MHD flow of a chemically reacting fluid past an impulsively started vertical plate with radiation, International Journal of Advances in Applied Mathematics and Mechanics (IJAAMM). 1(2)(2013) 1-15.
[33] E. M. Sparrow, H. S. Yu, Local non-similarity thermal boundary layer solutions, J. Heat Transfer. 93(1971) 328-334.

[34] S. Sengupta, N. Ahmed, MHD free convective chemically reactive flow of a dissipative fluid with thermal diffusion, fluctuating wall temperature and concentrations in velocity slip regime, Int. J. of Appl. Math and Mechl. 10(4)(2014) 27-54.